International Journal of Progressive Sciences and Technologies (IJPSAT)
ISSN: 2509-0119.
© 2022 Scholar AI LLC.
Vol. 32 No. 2 May 2022, pp. 350-358

Design And Analysis of An Innovative Wind Flow Accelerator for Wind Devices

MOUMOUNI GUERO Mohamed[1-2-3-]*, PRODJINONTO Vincent[1-2]

[1]Department of Mechanical and Energy Engineering, Polytechnic School of Abomey-Calavi, Republic of Benin.
[2]Laboratory of Energetics and Applied Mechanics, University of Abomey-Calavi, Republic of Benin.
[3]University Institute of Technology, Dan Dicko Dankoulodo University of Maradi, UDDM, Republic of Niger.

(cc) BY

Abstract – Scientists are increasingly interested in finding ways to optimize renewable energy sources. Among these renewable energies, wind energy is the most promising after solar energy. However, these wind resources are highly localized. This study proposes a flow accelerator called a convergent, capable of integrating with a wind device to increase its performance at low wind speeds. This convergent is designed in Solidworks and analyzed using Autodesk CFD. Three cases of inlet parameters were simulated, namely, inlet velocity of 3m.s^{-1}, 6 m.s^{-1} and 10 m.s^{-1}. The results of simulations showed a drop of the absolute pressure at the outlet and a multiplication of the velocity of the order of 11.5 times. These results agree with the demonstrated mathematical argument and validate the principle of conservation of volume flow. It is concluded that the combination of convergent and a wind device generates higher mechanical powers and thus a better electrical energy production.

Keywords – Flow Convergent, Low Wind Speed, Computational Fluid Dynamics, Autodesk CFD, Vertical Axis Wind Turbine.

I. INTRODUCTION

After solar energy, wind has emerged as the second most promising renewable energy resource. A wind turbine may convert wind energy into mechanical energy and ultimately into electrical energy. This natural resource is not evenly distributed on the planet, and there are regions that are moderately or extremely badly winded. To exploit this energy in these places, one must enlarge the wind device by extending the length of the blades and go to extremely towering heights, which frequently creates structural concerns.

Many scientists have been working to develop innovative wind turbines that are able to cope with the problems faced by existing wind turbines. They have developed turbines that are adapted to the site, reduce noise and weight. F. Wenehenubun et al [1] found that the three-blade wind turbine produces higher rotational speed and peak speed ratio. K. Pope et al [2] developed a vertical axis wind turbine (Zephyr) that has an external stator and an internal rotor. Their work established an empirical correlation that characterizes the operating performance of a vertical axis wind turbine. N. Koprasertsak et al [3] developed a wind booster having curved guide vanes that guide the wind flow and accelerate it to the blades. With this device, the power coefficient increases more than what is obtained with straight guide vanes for the same low wind speed and top speed ratio. D. Kim and Gharib [4] studied the effect of adding an upstream deflector on the power output of a vertical axis wind turbine. In an experimental study, they determined that the power output depends on the size and relative position of the deflector. M. Takao et al [5] developed an airflow control device called a " Directed-Guide-Vane-Row ". This straight blade mechanism is inherently limited due to its design; it can only capture a wind flow in one direction. W.T. Chong et al [6] conceived omnidirectional guide vanes, which can considerably raise the power output of a vertical axis wind turbine. Shikha TS et al [7] used a convergent nozzle in the upstream flow to reduce negative moments and improve effective wind speed. Mohamed MH, et al [8] positioned a windscreen at an angular position in the upwind to prevent negative moment on the backing wind turbine blade. J. K. Sharma et al [9] have designed and assessed a new type of wind booster. This booster which is a combination of a concentrator and a deflector, concentrates the flow towards the front blade and deflects the flow from the rear blade area. The result is that the angular velocity

Corresponding Author: MOUMOUNI GUERO Mohamed

of the wind turbine with booster has increased significantly, which leads to an increase in the mechanical performance of the three-blade wind turbine. E. Douvi et al [10] proposed an innovative design of wind device named "KIONAS". It is composed mainly of a rotor which is enclosed by a stator. Their analysis shows that the power output of the wind turbine increases with the diameter and number of blades.

This research discusses a wind flow accelerator that may be inserted in a wind turbine to improve its performance. Fundamentally, this accelerator offers numerous benefits that help in enhancing the turbine's performance. For starters, it greatly boosts wind speed at the output due to its design, which favors flow conservation in a pipe. It also converges airflow directly onto the leading blade, resulting in a stronger rotational moment of the turbine and, as a result, increased efficiency. The document is essentially structured around three sections, namely the mathematical method and modeling of the flow accelerator, the CFD simulation and analysis of the results achieved, and finally the concluding remarks of the research.

II. MATERIALS AND METHODS

This section outlines the mathematical equations that led to the choice of the wind flow accelerator. A corresponding mechanical model is proposed and submitted to a numerical analysis to evaluate its performance. However, before elaborating on the mathematical methods that helped in the choice of the accelerator, it is essential to clarify its use on the wind device.

The accelerator is arranged in such a way that it concentrates the wind flow directly onto the blades. These blades are designed to receive the flow perpendicularly to their straight section. They will be coupled to a disk attached to a motor shaft. This wind flow will exert a pressure on the blades and thus drive in rotation the motor disk. This movement will be transmitted from the motor shaft to a generator via an appropriate mechanism. A speed multiplier is used as the transmission mechanism.

2.1. The mathematical methods for designing the wind flow accelerator

The power available at a classical wind system is given by the expression:

$$P_{recoverable} = 1/2\ \rho A U^3 \quad (1)$$

where $P_{recoverable}$ is the wind power (W), ρ is the air density (kg/m^3), A is the frontal area (m^2), and U is the wind speed (m/s).

This expression can be written in the equivalent form:

$$P_{recoverable} = \frac{E_c}{t} = 1/2\ \dot{m} U^2 \quad (2)$$

With Ec: kinetic energy; t: time and $\dot{m}$: volume flow rate.

In this equation, the power increases as the speed U increases.

The idea behind the accelerator is to canalize the air flow in a pipe and to convey it directly to the blades of the wind turbine. This system must first accelerate the wind speed and above all project the wind flow directly onto the turbine blades, which will exert an intense pressure and thus turn the blades faster. It is possible to accomplish this by utilizing the principle of volume flow conservation in a pipe. A fluid flowing in a pipe with cross-sectional area A is characterized by its volume flow rate $\dot{m}$. The velocity U of the fluid flow and the cross-sectional area of the pipe affect this volume flow rate. The volume flow rate is conserved along the pipe, i.e., it is the same through all sections of the pipe. The consequence of this conservation is that the flow velocity of the fluid is not the same at all points; it depends on the value of the cross section of the pipe. From the inlet of the pipe to its outlet, the following equation is derived :

$$U_1 * A_1 = U_2 * A_2 \Rightarrow U_2 = U_1 * \frac{A_1}{A_2} \quad (3)$$

The *Barré de Saint-Venant* equation that applies to irreversible processes can be established as follows:

$$\frac{T_0}{T} = 1 + \frac{\gamma - 1}{2} M_0^2 \quad (4)$$

This equation has the benefit of relating the total temperature to the Mach number at any point in the flow. It also allows linking other variables to the Mach number:

$$\frac{P_0}{P} = \left(1 + \frac{\gamma - 1}{2} M_a^2\right)^{\gamma/\gamma - 1} \quad (5)$$

$$\frac{\rho_0}{\rho} = \left(1 + \frac{\gamma - 1}{2} M_a^2\right)^{1/\gamma - 1} \quad (6)$$

$$\frac{a_0}{a} = \left(1 + \frac{\gamma - 1}{2} M_a^2\right)^{1/2} \quad (7)$$

Critical conditions can be defined as those that prevail at a point in the flow where the velocity is sonic, that is, when $M_a = 1$. The critical quantities will be noted with an asterisk. They are easily deduced from the previous relations by posing $M_a = 1$.

$$\frac{T^*}{T_0} = \frac{2}{\gamma + 1} \quad (8)$$

$$\frac{P^*}{P_0} = \left(\frac{2}{\gamma + 1}\right)^{\gamma/\gamma - 1} \quad (9)$$

$$\frac{\rho^*}{\rho_0} = \left(\frac{2}{\gamma + 1}\right)^{1/\gamma - 1} \quad (10)$$

$$\frac{a^*}{a_0} = \left(\frac{2}{\gamma + 1}\right)^{1/2} \quad (11)$$

It should also be noted that the critical velocity is identified with the critical sound velocity which depends only on the temperature in the generating state of the gas.

$$U^* = a^* = \left(\frac{2\gamma}{\gamma + 1} r T_0\right)^{1/2} \quad (12)$$

In equation (5), assuming $n = \gamma/\gamma - 1$ and $x = \frac{\gamma}{\gamma - 1} M_a^2$, and by conducting a limited development of order 2, the resulting equation is obtained:

$$P_0 - P = \frac{1}{2}\rho U^2 \left(1 + \frac{M_a^2}{4} + O(M_a^4)\right) \quad (13)$$

Thus, the Bernoulli equation appears as a second-order limited development of the Saint-Venant equation with a margin of error of $\frac{M_a^2}{4}$ which is 1% when $Ma = 0.2$ and 6% when $Ma = 0.4$.

From the above, when $Ma < 0.3$, a compressible fluid can reasonably be considered an incompressible fluid:

$$P_0 \cong P + \frac{1}{2}\rho U^2 \quad (14)$$

In the incompressibility limit stated above, the mass flow rate $(\dot{m})$ is written:

$$\dot{m} = A P_0 M_a \left(\frac{\gamma}{r T_0}\right)^{1/2} \left(1 + \frac{\gamma - 1}{2} M_a^2\right)^{(\gamma + 1)/(2 - 2\gamma)} \quad (15)$$

A maximum velocity of the flow that results from the expansion of the gas to vacuum $(P = 0 \Rightarrow T = 0)$ is given by:

$$U_{max} = (2 C_p T_0)^{1/2} = a_0 \left(\frac{2}{\gamma - 1}\right)^{1/2} \quad (16)$$

Using the equations of celerity of sound and momentum, the following equality is found:

$$M_a^2 \frac{dU}{U} = -\frac{d\rho}{\rho} \quad (17)$$

Interpretation of equation (17) with respect to a subsonic flow $(Ma < 1)$

$|dU / U| > |d\rho / \rho| \Rightarrow \rho U$ follows the variation of U, so $\rho UA = cte \Rightarrow$ decrease of A, hence convergent.

Interpretation of equation (17) with respect to a subsonic flow $(Ma > 1)$

$|dU / U| < |d\rho / \rho| \Rightarrow \rho U$ follows the variation of ρ, so $\rho UA = cte \Rightarrow$ increase in A, hence the divergent feature.

Combining equation (17), mass conservation and the logarithmic form of $d(\rho UA) = 0$, the Hugoniot relation is determined :

$$\frac{dA}{A} = (M_a^2 - 1)\frac{dU}{U} \quad (18)$$

Interpreting the equation (18), from the sonic perspective $(Ma = 1)$:

$dA = 0$ which leads to a cylindrical pipe

$dU/U \rightarrow \infty$ which reasonably leads to $dA \approx 0$

so logically there exists for the sonic case $(Ma = 1)$ a minimal or critical section (A^*) where flow conservation is possible.

In synthesis, the adequate device to increase the speed is a convergent with a minimum critical section. This minimum critical section must be chosen so that the Mach number does not exceed the value of 1; this will avoid the problems of shock waves and turbulences.

The conservation of mass between these two sections leads to:

$$\frac{A}{A^*} = \frac{1}{M_a}\left[\frac{2}{\gamma+1}\left(1 + \frac{\gamma-1}{2}M_a^2\right)\right]^{\frac{\gamma+1}{2\gamma-2}} \quad (19)$$

From equation (19), once the inlet velocity is known, the Mach number (Ma) is determined and thus the right-hand side member is known once the gas in operation is known. The designing of the convergent is completed by choosing the inlet cross section (A) and deducing the critical cross section (A^*) by calculation.

From the conservation of flow, a relationship is established between the velocity of the fluid at any point and the critical velocity:

$$\frac{U}{U^*} = \left(\frac{2}{\gamma+1}\right)^{\frac{1}{\gamma-1}}\left(1 + \frac{\gamma-1}{2}M_a^2\right)^{\frac{1}{\gamma-1}} M_a\left[\frac{2}{\gamma+1}\left(1 + \frac{\gamma-1}{2}M_a^2\right)\right]^{-\frac{\gamma+1}{2\gamma-2}} \quad (20)$$

Similarly, the maximum critical flow rate is written:

$$\dot{m}_{max} = \rho^* A^* U^* = \rho_0 A^* a_0 \left(\frac{2}{\gamma+1}\right)^{\frac{\gamma+1}{2\gamma-2}} \quad (21)$$

2.2 Design and modeling

The flow accelerator is designed such that it channels the wind from its inlet section to the outlet section. The principle of conservation of volume flow requires us to vary both sections to increase the output velocity. Based on the mathematical reasoning in section 2.1, the mechanical model, called flow convergent, shown in figure 1 is chosen. This model is made with SolidWorks 2020. The material used for the modeling is galvanized steel. The geometric parameters of the wind flow accelerator are shown in Table 1.

Table 1: Geometric parameters of the wind flow convergent

Parameter	Value (mm)
Inlet diameter	D = 600
Outlet diameter	d = D/3 = 200
Length	L = 1000
Sheet thickness	e = 2

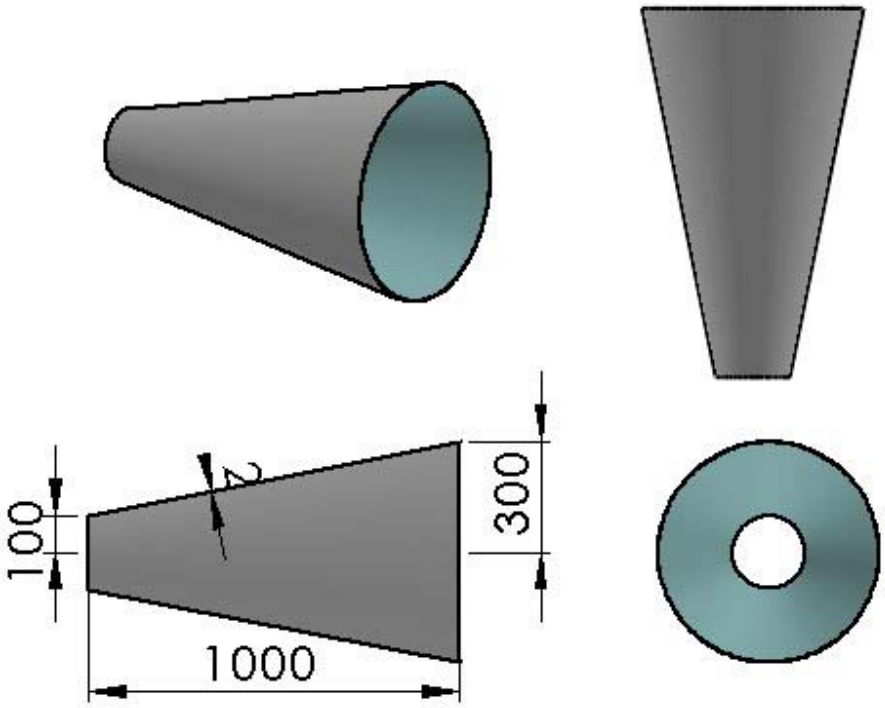

Figure 1: Mechanical model of the flow convergent

The figure below depicts the arrangement of the various parts of the new wind turbine layout as well as the best setup of the flow accelerator.

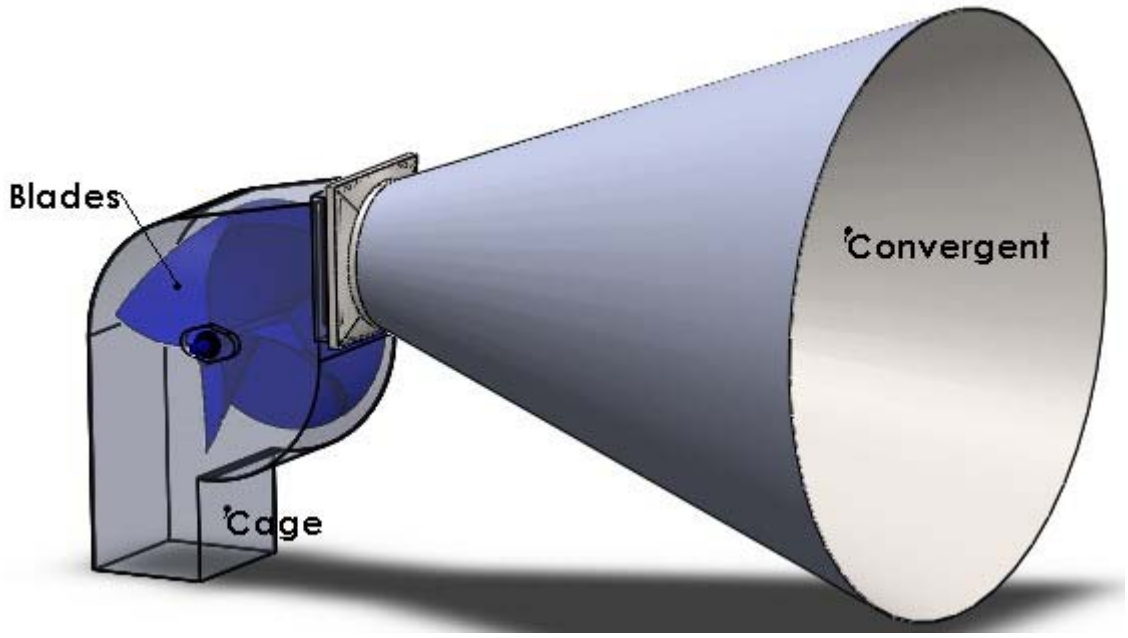

Figure 2: Location of the flow convergent in alignment of the blades

Figure 2 shows the positioning of the convergent with respect to the wind device. The blades of the device are placed in a cage whose main air inlet is the outlet of the convergent. This cage will avoid the wind tunneling phenomenon, and in the end the only source of air inlet to the wind device is the convergent outlet.

The following analysis allows us to determine the values of the convergent outlet flow. The wind speeds at the convergent outlet are applied directly to the blades to rotate them.

2.3. Numerical analysis of the wind flow convergent

To compute various properties of a fluid such as pressure, velocity, and flow rate in a flow system, the continuity equation and the Navier-Stokes equation must be solved for conservation of mass and conservation of momentum in the fluid flow. These equations are solved with a numerical solution using discrete interval boundary conditions. Autodesk CFD is used in this study for the numerical solution. It uses the Finite Volume Method (FVM) discretization solver to solve the boundary flow equations for the volumetric surface of a small volume element on a mesh geometry. The governing equations are given by the following expressions in differential form: A. M. Malge, P. S. Kalos [11].

Continuity equation

$$\frac{\partial \rho}{\partial t} + \vec{\nabla}.(\rho \vec{V}) = 0 \quad \textbf{(22)}$$

Equation of momentum

$$\frac{\partial (\rho \vec{V})}{\partial t} + \vec{\nabla}.(\rho \vec{V}\vec{V}) = \vec{\nabla}.P + \rho \vec{g} = -\vec{\nabla}p + \vec{\nabla}.\Sigma + \rho \vec{g} \quad \textbf{(23)}$$

Equation of energy

$$\frac{\partial (\rho E)}{\partial t} + \vec{\nabla}.(\rho E \vec{V}) = \vec{\nabla}.(P.\vec{V}) + \rho \vec{g}.\vec{V} + \vec{\nabla}.\vec{q} + \vec{\nabla}.\overrightarrow{q_R}$$

The six-degree-of-freedom solver uses the forces and moments of the object to calculate the translational and angular motion of its center of gravity. The equation for the translational motion and rotational motion is given below: J. K. Sharma et al [9].

$$\dot{\vec{v_g}} = \frac{1}{m} \sum \vec{f_g}$$

With: $\dot{\vec{v_g}}$ is the translational motion of the center of gravity, m is the mass, and $\vec{f_g}$ is the force vector due to gravity.

$$\dot{\vec{\omega_B}} = L^{-1}\left(\sum \vec{M_B} - \vec{\omega_B} \times L\vec{\omega_B}\right)$$

Where: L is the inertia tensor, $\vec{M_B}$ is the body moment vector, and $\vec{\omega_B}$ is the rigid body angular velocity vector.

The boundary conditions used for the calculation is the constant inlet velocity V = (3m.s^{-1}, 6m.s^{-1} and 10m.s^{-1}) at atmospheric pressure. The outlet pressure is considered as an absolute pressure. A tetrahedral mesh is used for the whole analysis. The mesh used is an unstructured tetrahedron. The reference values are given from the convergent input and are shown in Table 2.

Table 2: Reference values for simulation

Density (Kg/m^3)	Viscosity (Kg/m-s)	Surface (m^2)	Température (K)	Velocity (m/s)	Pressure (Pa)
1,292	18,5 x 10^{-6}	0,2826	300	3 - 6 - 10	101325

III. RESULTS OF THE ANALYSIS

The numerical analysis of the flow convergent is performed by Autodesk CFD. A detailed study of the pressure and velocity variation inside the convergent has been simulated. This will allow evaluating its output performance and to appreciate the changes in velocity and pressure. For this simulation, three different velocity cases are evaluated. The results of this simulation are illustrated in the following figures.

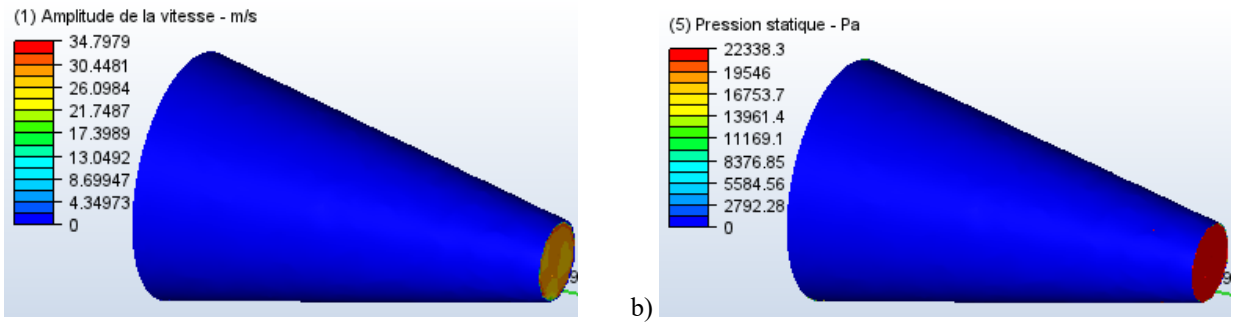

a) b)

Figure 3: Velocity amplitude (a) and pressure (b) at the outlet of the flow convergent for an inlet velocity of 3 m.s^{-1}

From the analysis of Figure 3 (a and b), we can see that the flow convergent is simulated for an input wind speed of 3 m.s^{-1}. The total number of nodes for the mesh is 283573. It is observed that for input velocity values of 3 m.s-1, there follows a multiplication of the output velocity values of the order of 11.6 times to reach therefore 34.4 m.s^{-1}. The value of the absolute pressure at the outlet declines to 22338.3 Pa.

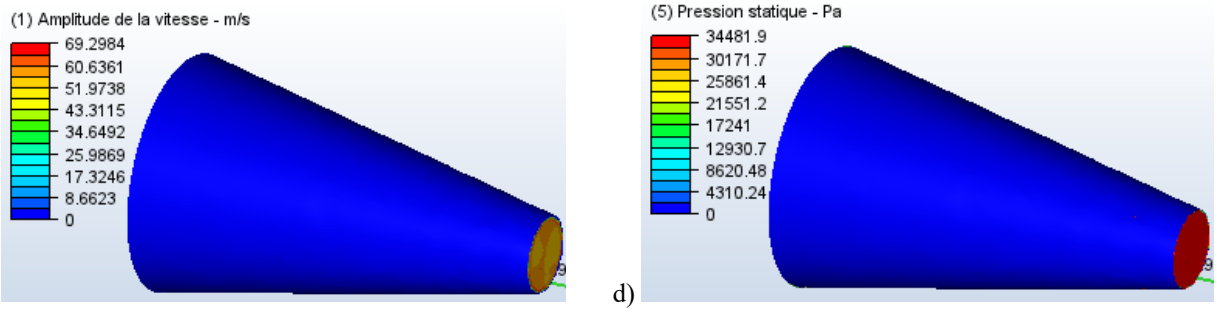

c) d)

Figure 4: Velocity amplitude (c) and pressure (d) at the outlet of the flow convergent for an inlet velocity of 6 m.s^{-1}

Figure 4 (c and d) shows the evolution of the performance parameters for an inlet velocity of 6 m.s^{-1}. Figure 4-c shows that the velocity reaches a maximum threshold of 69.3 m.s^{-1}, while Figure 4-d shows the equivalent outlet pressure at 34481.9 Pa.

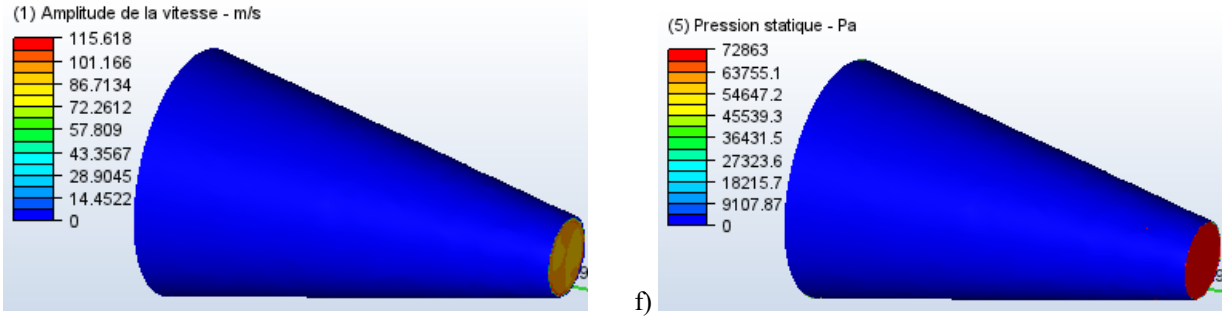

e) f)

Figure 5: Velocity amplitude (e) and pressure (f) at the outlet of the flow convergent for an inlet velocity of 10 m.s^{-1}

Figure 5 (e and f) shows the pressure and velocity evolution for an inlet velocity of 10 m.s^{-1}. The pressure at the outlet drops to 72863 Pa, while the velocity reaches a maximum of 115.6 m.s-1, i.e., a multiplication of 11.5 times.

IV. DISCUSSIONS

The convergent is simulated for velocity and absolute pressure parameters. The analysis of Figures 3, 4 and 5 provides information on the expected performance of the flow convergent. The variation of the parameters from input to output is quite meaningful. It can be easily noticed that the speed at the outlet of the convergent is multiplied by an average of 11.5 in all cases of the study. This proves that the proposed device is indeed a speed multiplier. Obviously, the use of the convergent on a wind device will allow generating higher mechanical powers and thus a much better production of electrical energy.

According to the dimensional configuration of the proposed convergent, it is clear that any desired level of multiplication can be achieved. To do so, it is sufficient to adjust the dimensions of the inlet section and the outlet section; the ratio of the sections being the multiplier of the inlet velocity to find the outlet velocity according to the principle of conservation of volume flow.

These results are in accordance with the research of Shikha TS et al [7] whose works led to the design of convergent nozzles to channel and accelerate the wind. We also note the study done by N. Koprasertsak, et al [3] on the design of guide valves to regulate the direction of the flow and accelerate it in all directions to produce impacts on the blades of vertical axis wind turbines.

V. CONCLUDING REMARKS

An innovative flow accelerator, called convergent, has been designed to increase the wind speed for wind devices. Three different cases of input parameters were modeled, namely, input velocity of 3m.s^{-1}, 6 m.s^{-1} and finally 10 m.s^{-1}. The performance analysis of the convergent was done for the outlet pressure and velocity parameters.

A mathematical reasoning guided in the choice of the shape of the accelerator: the choice fell on a convergent with a minimal output section so that the Mach number does not exceed one. The mechanical model was created on SolidWorks and its performance analysis was done in Autodesk CFD. As a result, one observes in all three cases of simulation:

A multiplication of wind velocity at the outlet of the convergent approximately 11.5 times the input velocity. This is very satisfactory compared to the desired results.

A decrease of the absolute pressure at the outlet of the tested convergent.

These convergent output parameters, when combined with a wind turbine, will produce a higher mechanical efficiency, which significantly improves electrical energy production.

Nevertheless, it will be necessary to continue the research and improve the convergent based on different parameters such as its design, length, profile curves, positioning in respect to the location of the wind device, etc.

The future works are focused on the manufacturing of the prototype of wind device able to receive the flow convergent to improve its production capacities. The design and simulations of the prototype are already done. At the end of the implementation and performance tests, a comparative analysis will be done to confirm the results. These results will be published in a future article.

NOMENCLATURE

Ma = Mach number

P_0, V_0, T_0, ρ_0 = Generative state parameters

a = Velocity

t = Time (s)

ρ = Density of the fluid (kg.m-3)

$\vec{V}$ = Eulerian velocity of a fluid particle (m.s-1)

P = stress tensor (or pressure tensor)

p = thermodynamic pressure (Pa)

$\vec{g}$= gravity (m s^{-2})

E = total energy per unit mass (J.kg^{-1})

I = unit tensor

Σ = viscous stress tensor (Pa)

$\vec{q}$= heat flux due to thermal conduction (J.m-2 s^{-1})

$\overrightarrow{q_R}$= heat flux due to radiation (J.m-2 s^{-1})

ACKNOWLEDGMENTS

The work described in this paper was partially supported by the University Institute of Technology of University Dan Dicko Dan Koulodo of Maradi, Republic of Niger and the Laboratory of Energetics and Applied Mechanics of the University of Abomey Calavi, Republic of Benin. May they find our sincere thanks.

AUTHOR CONTRIBUTIONS

Moumouni Guero Mohamed conceived, designed, and performed the experiments; Moumouni Guero Mohamed analyzed the data; PRODJINONTO Vincent contributed materials and analysis tools. Moumouni Guero Mohamed authored the paper.

CONFLICTS OF INTEREST

The authors declare no conflicts of interest. The sponsors had no role in the design of the study; analyses or interpretation of data; in the writing of the manuscript, and in the decision to publish the results.

REFERENCES

[1] F.Wenehenubun, A. Saputra, H.Sutanto, “An experimental study on the performance of Savonius wind turbine related with number of blades,” Energy Procedia 68 (2015) 297-304
[2] http://creativecommons.org/licences/by-nc-nd/4.0/
[3] K. Pope Rodrigues, R. Doyleab, T. Sopelas, R. Gravelsins, G.F. Naterer, E. Tsang, “Effects of stator vanes on power coefficients of a zephyr vertical axis wind turbine,” Renewable Energy, 2010, 35, 5, pp. 1043-1051.
[4] N. Korprasertsak, T. Leephakpreeda, “Optimal Design of Wind Boosters for Low-Speed Vertical Axis Wind Turbines,” Applied Mechanics and Materials, ISSN:1662-7482, Vol. 798, pp 195-199
[5] https://doi.org/10.4028/www.scientific.net/AMM.798.195
[6] D. Kim, M. Gharib, “Efficiency improvement of straight-bladed vertical-axis wind turbines with an upstream deflector,” J. Wind Eng. IndAerodyn. 115 (2013) 48-52 DOI: 10.1016/j.jweja.2013.01.009
[7] M. Takao, H. Kuma, T. Maeda, Y. Kamada, M. Oki, A. Minoda, “A Straight-Bladed Vertical Axis Wind Turbine with a Directed Guide Vane Row – Effect of Guide Vane Geometry on the performance,” Journal of Thermal Science. 2009; 18(1): 54-57 DOI: 10.1007/s11630-009-0054-0
[8] W. T. Chong, S. C. Poh, A. Fazlizan, K. C. Pan, “Vertical Axis Wind Turbine with Omni-Directional-Guide-Vane for Urban High- Rise Buildings,” Journal of Central South University. 2012; 19: 727-732
[9] DOI: 10.1007/s11771-012-1064-8
[10] Shikha TS, Kothari DP, “Wind energy conversion systems as a distributed source of generation,” ASCE Journal of Energy Engineering 2003; 129(3):69-80 https://doi.org/10.1061/(ASCE)0733-9402(2003)129:3(69)
[11] Mohamed MH, Janiga G, Pap E, Thevenin D, “Optimization of Savonius turbines using an obstacle shielding the returning blade,” Renewable Energy 2010; 35(11) :2618-26
[12] https://doi.org/10.1016/j.renene.2010.04.007
[13] J. K. Sharma, A. Goyal, M. Pandey & S. Kumar, “Design and analysis of vertical axis wind turbine booster at low wind speed,” International Journal of Mechanical and Production Engineering Research and Development (IJMPERD); Vol. 10, Issue 3, Jun 2020, 13823-13836
[14] E. Douvi, D. Douvi, D. Margaris, I. Drosis, “Numerical and Computational Analysis of a New Vertical Axis Wind Turbine, Named KIONAS,” Computation 2017, 5(1),8.
[15] A. M. Malge, P. S. Kalos, “Numerical Analysis of Innovative Wind Booster Configurations for Vertical Axis Wind Turbines,” International Journal of Recent Technology and Engineering (IJRTE); Volume-9 Issue-1, May 2020. DOI:10.35940/ijrte.A1214.059120